RSC Sustainability

ROYAL SOCIETY OF CHEMISTRY

PAPER

View Article Online
View Journal | View Issue

Cite this: *RSC Sustainability*, 2023, **1**, 1233

Hollow silica nanoparticles loaded with industrial dyes for high exhaustion leather dyeing and its sustainability impact†

Sathya Ramalingam, *[a] Jonnalagadda Raghava Rao [b] and Kalarical Janardhanan Sreeram [c]

Nowadays, it is difficult to maintain acceptable water quality owing to dye pollution caused by rapid industrialization. Coloured dye discharge from the leather dyeing process has numerous anthropogenic effects on water sources. Synthetic leather dyes can be considered environmental pollutants because of their toxicity, and mutagenic and carcinogenic effects. Hence, there is an increasing demand to develop a high-exhaustion dyeing process without influencing leather quality. In this study, high dye exhaustion was attempted using hollow nanoparticle-stabilised industrial dyes, which are the most interesting liquid dyes in the context of sustainable dyeing. A simple method of preparing dye-modified hollow silica nanoparticles for better binding with leather has been reported using silica with hydroxyl and acrylate groups. The optimum condition for maximum dye uptake was obtained at pH 5.5–6, 90 min of drumming and 25–30 °C. Further, the effect of changes in the nanoparticle surface functional groups, particle size and type of tanned leather for dyeing were evaluated. The hollow spheres model with acrylate groups showed good dyeing characteristics with 98% dye uptake by applying the leather matrix. Compared to the conventional dyeing process, the E factor (environmental factor) of the new way of dyeing by hollow nanoparticles was estimated to be lower (at a value of 0.35), indicating minimum emissions and less pollution load. The economic viability of the newer dyeing system was also analysed through a cost-benefit analysis. A high exhaustion (high uptake) dyeing system is a sustainable alternative to conventional dyeing, providing a fundamental and innovative contribution. Thus, nanotechnology offers a technology that can be used as a tangible solution for coloured discharge in leather processing. As per the sustainability goal (goal 6), this new dyeing system was related to the ethical imperative of providing humanity with a minimum standard of living (affordable clean water by minimum dye discharge).

Received 4th March 2023
Accepted 29th May 2023

DOI: 10.1039/d3su00079f

rsc.li/rscsus

Sustainability spotlight

According to the sustainable development goals, the avoidance of auxiliaries and the discharge of coloured water position this discussion under the topic of clean water and sanitation (SDG 6). The conventional method of colouring in the leather industry discharges an enormous amount of toxic chemicals, such as unfixed dyes, salts, and toxic metals. The green chemistry approach to attain sustainable colouring (reduction in 40–50% of dye load in wastewater) using hollow silica-embedded industrial dyes as dyeing agents is reported in this study. *Greener impacts*: (i) to establish the potential for advanced sustainable processes in the present leather science using cost-effective dye-modified silica nanoparticles as dyeing agents. (ii) Complete elimination of hazardous chemicals, such as dye levelling agents, cationic fixing agents, dye penetrators, and dye fixing agents, such as acid and alkali. (iii) High exhaustion dyeing system using dyes modified with silica. (iv) Sustainability assessments, such as E-factor and mass intensity evaluation, identify the silica-based dyeing process as greener than the conventional system. (v) Good softness with improved strength properties obtained for silica-treated leathers is compared to the free dye system.

Introduction

The dyeing process for leather consumes large amounts of water, dyes and chemicals (which ensure the leather's colour) in addition to auxiliaries (chemicals that aid colouration).[1] At the end of colouration, the unfixed dye spent chemicals, auxiliaries and the water not absorbed by the fibre material are discharged as effluent.[2] These effluents, typically coloured, adversely impact aquatic life if discharged without treatment.[3]

[a]*Leather Process Technology Department, Central Leather Research Institute, Adyar, Chennai 600 020, India. E-mail: leathersathya@gmail.com; rsathya@clri.res.in; Tel: +91 44 24437230*

[b]*Inorganic and Physical Chemistry Laboratory, Central Leather Research Institute, Adyar, Chennai 600 020, India*

[c]*Central Leather Research Institute, Adyar, Chennai 600020, India*

† Electronic supplementary information (ESI) available. See DOI: https://doi.org/10.1039/d3su00079f

Consequently, riverbeds, soil and crops are affected by such effluents.[4] With this unfriendly relationship to the natural environment, leather colouration can fully utilize the eco-conservation trend.[5]

Water bodies, such as lakes and rivers, which contain minimal amounts of dyes (<1 ppm), contribute to damaging the aquatic environment through the reduction of aesthetic quality and transparency.[6] Leather can be coloured using natural dyes, synthetic dyes, or a combination.[7] Accordingly, synthetic dyes make up 90% of the dyes used in leather dyeing.[8] An azo group is a significant component of most synthetic anionic dyes.[9] Azo dyes endanger water quality and supply because of their non-degradability, toxicity, and accumulation of unreacted monomers in wastewater.[10] Highly coloured azo dye discharges produce carcinogenic and mutagenic effects affecting aquatic life and humans. One of the most crucial steps in leather dyeing is choosing the appropriate dyes for colouring the leather matrix.[11] For example, leather tanned with positive chromium tends to bind with anionic dyes. However, in the case of the weakly positive charge, chromium-free tanned leather cannot strongly bind anionic dyes, resulting in low-quality dyed leather.[12] Depending on the type of tanning material, the sites available to react with dyes can also vary, resulting in various dyeing properties for the same dye. Convenient and low-priced acid dyestuffs have been used for dyeing mineral-tanned leather, owing to their brilliant colours, superior dyeing, and easy penetration, but the same dyes (anionic dyes) exhibit problems with fastness and consumption when dyeing vegetable-tanned leather.[13] For better dyeing properties in vegetable-tanned leathers, it is advisable to use 1 : 1 metal complex dyes that are known for their good light fastness, washing properties and good levelling capacities.[14] Further, using 1 : 1 metal complex dyes for vegetable-tanned leathers reduces dyestuff discharge to the environment and requires less treatment owing to their high consumption values.

Developing high-exhaustion liquid dyeing strategies is vital to ensure sustainability for future generations through newer technologies. Leather dyeing wastewaters are characterized by the enormous discharge of unreacted dyes, high chemical oxygen demand, biological oxygen demand, and total dissolved solids.[6] These discharges were due to the use of a huge quantity of chemicals at leather preparatory steps, such as tanning and post tanning. When discharged into the effluent, unfixed powder dyes and other monomers can pose severe environmental threats.[15] Many small-scale industries are susceptible to this problem due to the lack of cost-effective end-of-pipe treatment procedures. The quest for an eco-friendly dyeing process for leather is of paramount importance.[16]

The nanotechnology revolution is having an incredible impact on technology now and will do so in the future. Nanoparticles made of mesoporous silica (MSNP) are promising nanoengineered carriers that can carry many small molecules without any degradation.[17] Through layer-by-layer assembly, SiO_2 microparticles can be utilized as supports for the formation of vesicle-like particles.[18] Biocompatible silicon-based nanoparticles for leather dyeing remain unexplored. In general, silanes readily hydrolyze in an aqueous solution to form silanol groups (SiOH) that bind to various hydrated metal surfaces (metal–OH) through silicon (Si)–oxygen–metal bonds.[19] Furthermore, the silanol groups could self-crosslink *via* siloxane bonds (Si–O–Si), resulting in a chemically bound protective layer on the dye molecules. Organic dyes are usually functionalised with silica nanoparticles using one of two chemical methods.[20] The first strategy involves covalently attaching the dye to the silicates. However, the second method has been reported as entrapping the dye into the siloxane matrix using a noncovalent or non-bonding mechanism (*i.e.*, electrostatic interactions).[21] The presence of Si–AOH groups on the negatively charged surface of SiO_2 further impedes the adsorption of anions.[22] Surface functionalization or modification has been attempted to overcome these restrictions, with the goal of introducing functional groups that might affect silica nanoparticle chemical and physical characteristics.[23]

Modifying dyes with silica surfaces makes it easier to create new dyeing systems with tailored structures and functionalities in an aqueous solution.[24] Even recent research has focused on the synthesis of nanometric silica particles for tanning applications.[25] This is because of their small size and ability to interact with collagen fibers. Functional groups, such as thiols,[26] epoxy,[27] vinyl[28] and amines,[29] can be modified by introducing alkoxysilane derivatives.[30,31] The purpose of these functional groups is to neutralize or introduce a charge to surfaces, which provides advantages such as biocompatibility, supramolecular recognition or simply serving as reactive sites for protein interactions. For instance, silica nanoparticles with a size range of 10–200 nm have been shown to exhibit limited cytotoxicity in the field of drug carriers.[32] Hence, in this study, the commercial/industrial dyes used for colouring leathers were utilised for the preparation of silica nanoparticles. The dyes are surface functionalised using silica nanoparticles with surface functional groups of hydroxyls and methylacrylate. Conventional dye–leather interactions, such as electrostatic and hydrogen bonding by conventional dyes, are replaced by multiple hydrogen and covalent linkages by liquid dyes containing dyes modified with silica. Compared to conventional dyeing systems, this modification with silica increases the surface active group due to the narrow particle size of the dye molecules. There is increased exhaustion of the dyeing system achieved by dye modified with silica nanoparticles as a dyeing system. Therefore, the loading of dyes on silica polymers with different functionalities is a promising approach for protecting the environment by reducing coloured discharge. Because no auxiliaries were used, the environmental problems associated with dyeing auxiliaries were totally eliminated.

Materials and methods

Materials

All chemicals used were used as received from the supplier. Quinoline yellow dye with a content of 95% (CI number 47005), tetraethoxysilane (99%), silane A174 (99%), ammonium hydroxide (25%), and cationic surfactant, such as cetyltrimethylammonium bromide, were purchased from Sigma-Aldrich. Goat leather tanned with chromium and vegetable

tannins was utilised as a substrate for leather dyeing application. The chemicals used for leather making were of commercial grade. In laboratory experiments, analytical grade chemicals were used. Based on the shaved weight of goat leather, chemical percentages were offered.

Fabrication of dye modified OH terminated silica nanoparticles. In a double-neck round bottom flask, water and cationic surfactant were added to make micellar emulsions, as shown in Scheme 1. A solution containing 3.4 grams of cetyltrimethylammonium bromide was added slowly to 11.3 mL of the heptane under constant stirring for 12 minutes. To this surfactant mixture, add 7.65 grams of quinoline yellow dye. Constant stirring was maintained for 10 minutes to obtain a homogeneous coloured solution. To this solution, 103.3 grams of tetraethoxysilane was added and stirring continued for 10 minutes. To this solution, 0.33 grams of ammonia solution as a catalyst was added for 15 minutes. Then, the microemulsion was diluted with ethanol after allowing it to continue overnight under stirring. Water was used after ethanol washes to remove the free particles. In addition to dialysis, centrifugation was used to remove unreacted monomers. During dialysis, water was used as a medium for 12 h; for centrifugation, 12 000 rpm were applied for 15 min. Experimental triplicates were used to validate the method for forming silica nanoparticles, and the results showed that the method can be quantifiably reproduced.

Fabrication of dye modified with methylacrylate terminated silica nanoparticles. To create silica nanoparticles, trimethyoxysilyl propylmethacrylate was used as a precursor to generate methacrylate (acrylate)-terminated silica nanoparticles. Under continuous stirring, silane A174 (2.5 mL) was added dropwise into the homogeneous dye solution. To initiate the polymerisation process, 1.2 mL of NH_4OH was added to the reaction mixture. After stirring overnight, ethanol was added to break the microemulsion. The particles were washed a couple of times with ethanol and then washed with water. The sample codes of different silica nanoparticles containing different dyes and their corresponding descriptions are shown in Table S1.† All results were statistically evaluated using one-way ANOVA and a descriptive statistical test using the SPSS 15.0 statistical software package to determine the standard deviations of the averages. All data were represented as the mean for five independent measurements.

Instrumental methods. The optical properties of the dye-functionalised silica nanoparticles were investigated using UV-visible spectroscopy (PerkinElmer Lamba 35 spectrophotometer). The hydrodynamic diameter and polydispersity index (PDI) of an aqueous suspension of nanoparticles were measured by Dynamic Light Scattering (DLS) with a high-performance particle sizer (Zetasizer Nano series, Malvern) at 25 °C. The viscosity and refractive index of the dispersing medium (water) were fixed at 0.8825 cP and 1.33, respectively. Samples were prepared by dispersing 150 μL of the dye-modified silica nanoparticles in 2 mL of water (pH 6). Similarly, control dye solutions were prepared by dissolving 50 μL of 0.01 M dye solution in 2 mL of water (pH 6). A disposable polystyrene cuvette was used to measure the hydrodynamic diameter of the particles at 25 °C. The aqueous dispersant solution was subjected to filtration using PTFE (polytetrafluoroethylene) based 0.45 μm pore size filters before DLS measurements. The zeta potential of the sample in solution was determined through folded capillary cell ZEN 1070 and ZEN1002 Universal 'dip' cell. Z-averaged translational diffusion coefficients were calculated by applying the cumulant method.[33] To determine the nanostructure formation and morphology of the dye modified with silica nanoparticles, TEM was performed at 200 kV using JEOL 3010. The particles were properly washed and dispersed in ethanol before sample preparation. Changes in the surface functionality of the dye and functionalised dyes were studied using the FTIR spectrum. The spectrum of the sample was recorded using an ABB MB3000 Fourier transform infra-red (FTIR) spectrometer. All spectral analyses were performed with a resolution of 4 cm^{-1} and recorded at a 45° incident angle. The stability of dye-modified silica nanoparticles towards various temperatures was analysed by heating the dye solution (similar absorbance) gradually from 20 to 90 °C at an increasing rate of 1 °C min^{-1}. DLS (Zetasizer Nano series, Malvern) measurement of dye solution at various temperatures also studied the dye aggregation induced by temperature. Similarly, the pH-related properties were evaluated by adding various drops of diluted HCl (0.1 M) and NaOH (0.1 M) to the suspension to achieve the desired pH values. The particle size and zeta potential were determined. The experiment was carried out at 25 °C with water as a dispersant. The effects of acid and alkali on the physical characteristics of the unmodified and dye-modified silica nanoparticles were examined using DLS and UV-visible spectrophotometers. Dye-modified silica nanoparticles titrated against various concentrations of formic acid (0, 1.0, 2.0, 3.0, and 4.0 M)/alkali sodium bicarbonate (0, 0.5, 1.0, 1.5, and 2.0 M) were added, and the particle size was determined based on the different pH values. All of the experimental findings were statistically assessed using one-way

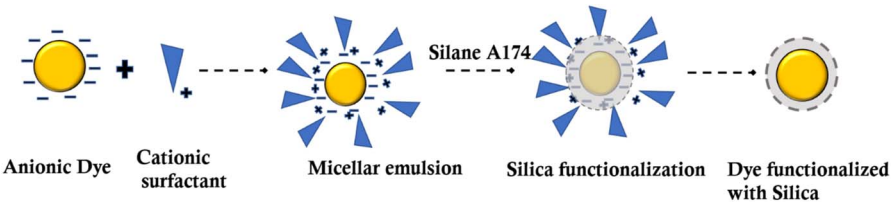

Scheme 1 Preparation of dye (quinoline yellow) functionalised silica nanoparticles.

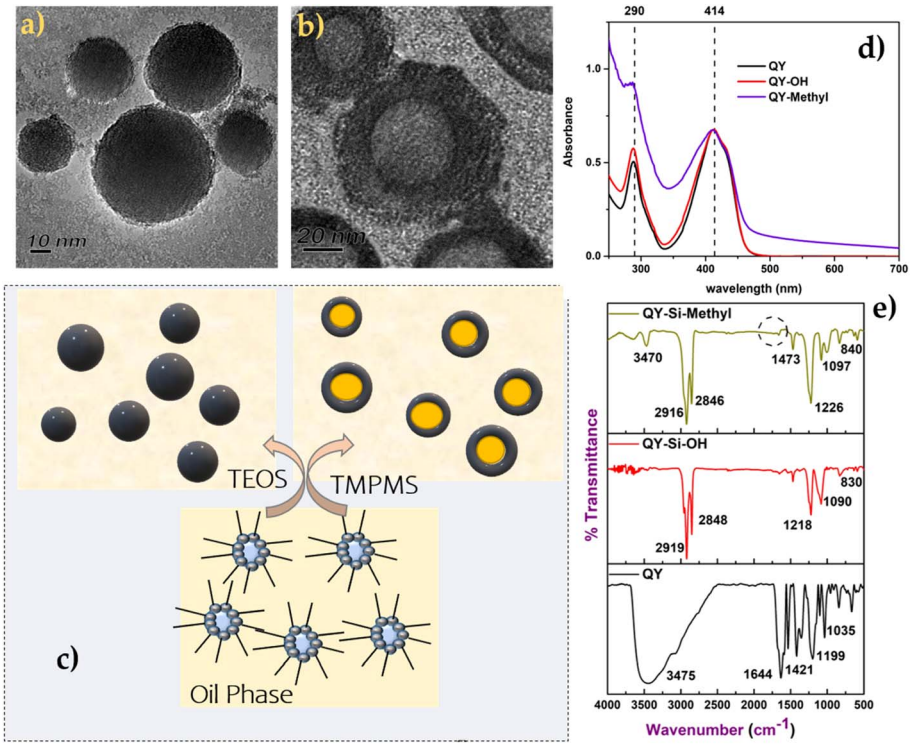

Fig. 1 (a) TEM image of dye-modified silica with a hydroxyl group, (b) the TEM image of the dye-modified silica nanoparticles with acrylate terminal, (c) schematic representation of the formation of different morphologies of dye-modified silica nanoparticles, (d) the excitation spectra and (e) the FTIR spectra of the dye compared with dye-modified silica nanoparticles.

Table 1 Dynamic light scattering measurement of the dye compared with dye modified with silica nanoparticles

Samples	Particle size (nm)	PDI	Zeta potential (mV)
QY	554 ± 23	0.483	−10.7 ± 0.2
QY-Si–OH	61 ± 5	0.326	−49.3 ± 0.9
QY-Si–acrylate	80 ± 3	0.112	−27.3 ± 0.25

ANOVA and descriptive statistical tests in the SPSS 15.0 statistical software program to estimate standard deviations of the averages. For five separate measurements, all data were expressed as a mean.

Crust leather dyeing process using conventional dyes and modified dyes. In the new dyeing, dye-modified silica nanoparticles were used instead of free dye. Each chrome and vegetable-tanned goat leather was divided into two halves along the backbone for matched pair comparison. For all dyeing trials, the anionic dye was used. The right half was chosen as the control, which was treated with free dye (unmodified quinoline yellow) (Fig. S1†), and the left half was considered to be experimental and used for treatment with dye-modified silica nanoparticles (QY-Si–OH and QY-Si–acrylate/methyl). Based on the w/v ratio, the material (shaved weight of leather) to the solution (dye solution) ratio was set at 1 : 10. Free dye (2%) and dye-modified silica nanoparticles (2%) were offered in equal amounts. The dyeing was carried out in a drum (rotating vessel) at 29 ± 2 °C for 45 min at a speed of 11 rpm (rotation per minute). The pH of the dye solution was found to be 7 after surface modification. After dyeing, the conventional treatment of retanning and fatliquoring was followed for both the control and experimental leathers, as depicted in Table S2.† A 2% dye levelling agent as dyeing auxiliaries was utilised in a conventional dyeing process. However, in the case of the dye-modified silica nanoparticle dyeing system, dyeing auxiliaries were avoided. Landmann 1989 reported that the skins were anisotropic in nature. Hence, all the samples were collected from the official sampling position[34] (OSP) (IUP 2000) for characterisation.[35]

Characterisation of dyed crust leather. The dyeing properties of the dyed crust leather dyed by free dyes and modified dyes were thoroughly investigated. Scanning electron micrographs were used to examine the surface morphology of the crust leather and composites (SEM with a Hitachi-SU6600 operating at 15.0 kV). The INSTRON universal testing machine was used to evaluate the crust leather's strength qualities (tensile and tear). Tanners assessed the dyeing qualities of both experimental and control crust leather, including dye uniformity and shade intensity L^*, a^*, and b^*differential dyeing. The leather porosity was determined using a PMI capillary flow porometer. A PerkinElmer Lamba 35 spectrophotometer was used to record the UV-vis absorption spectra of the samples. To analyse the silica distribution throughout the leather cross-section, an FEI Quanta 200 environmental SEM with an integrated EDX (energy-dispersive X-ray spectroscopy) detector was used to aid

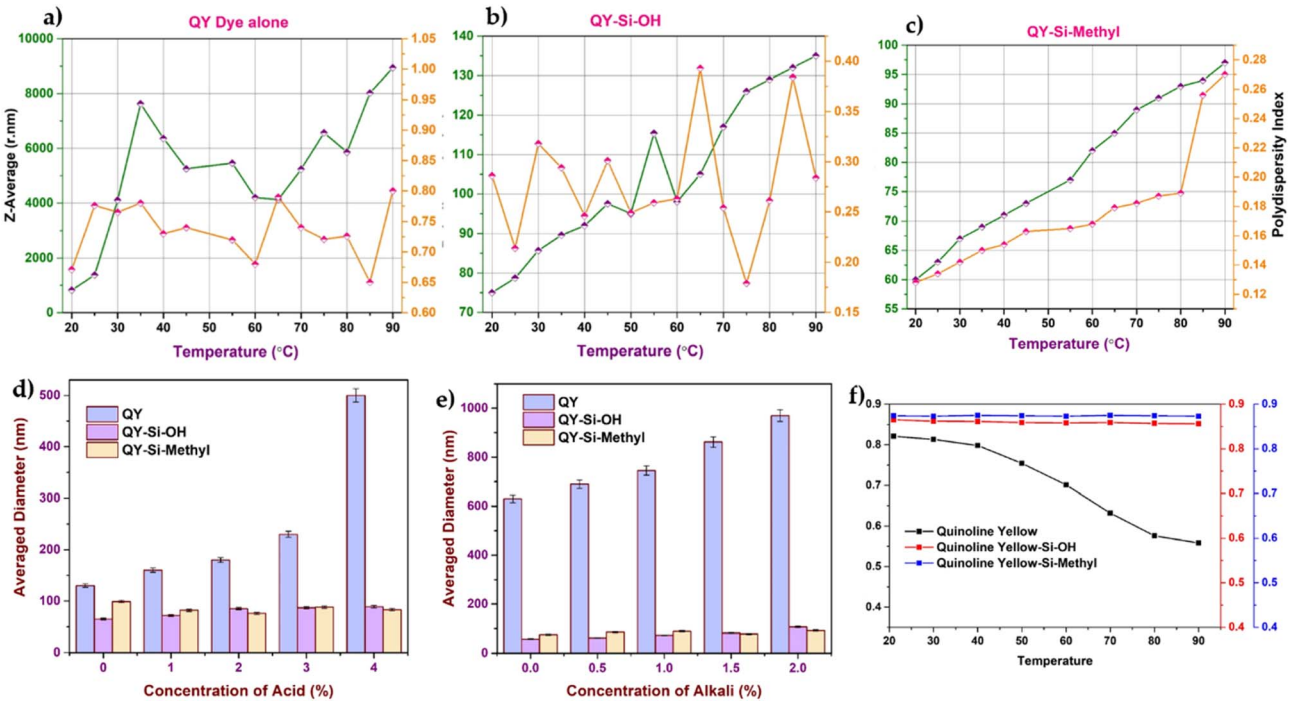

Fig. 2 Effect of temperature on average diameter and potential index of the (a) free dye and dye-modified silica nanoparticles with (b) hydroxyl terminal, and (c) acrylate/methyl terminal. (d) and (e) The stability of dyes against acid and alkali. (f) Degradation profile.

elemental analysis. Using a magnificent scope 5m USB digital microscope, surface and cross-sectional photographs of coloured leather samples were obtained. Colour stability against rubbing was analysed according to the standard methods of ISO 20433. The fastness test is pre-set for a certain number of rotations, and the colour degradation or transfer is subjectively determined using a greyscale. The softness of the leather samples was analysed by applying an ST 300 softness tester.

Results and discussions

Leather dyeing depends on the dye properties and the type of leather to be dyed. Drum dyeing with water-based liquid dyes has gained significant attention owing to their reduced aggregation of dye molecules and their reduced neutral salt concentration. Thus, liquid dyes can be preferred for dyeing applications based on their easy absorption by the leather matrix and reduction in the organic load in wastewater in the form of neutral salts. Hence, in this study, silica-based liquid dyes were prepared and used as dyeing agents in the dyeing of chrome and vegetable stabilised leather. Both chrome-tanned and vegetable-tanned leathers were dyed separately using the same dye to study dye uptake by different functional groups in silica (hydroxyl and methacrylate).

Preparation and characterisation of silica-based liquid dyes

The Transmission Electron Microscope (TEM) was used to examine the particle dispersity and morphology of the dye molecules. Fig. 1a and b reveal that the quinoline yellow formed the hollow model with acrylate terminal silica nanoparticles. The hollow silica with an acrylate terminal was formed, whereas

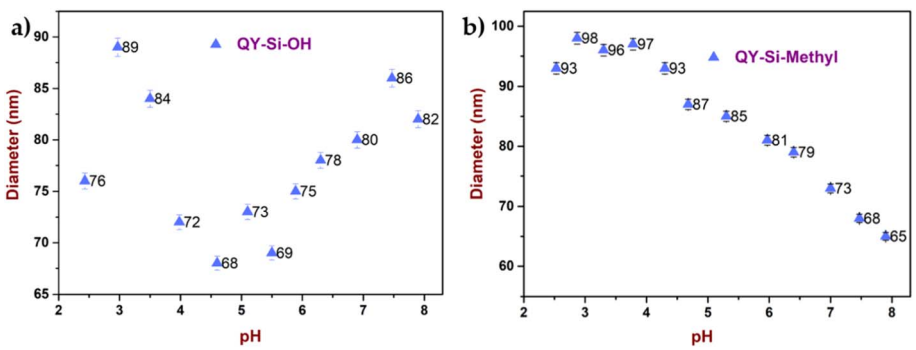

Fig. 3 Acid and alkali stability of dye-modified silica nanoparticles (a) with hydroxyl terminal and (b) methyl/acrylate terminal.

Table 2 Colour coordinate measurement of free and dye modified with silica nanoparticle-treated leathers[a]

Sample name		Grain side				Flesh side			
		L	a^*	b^*	ΔE	L	a^*	b^*	ΔE
Chrome tanned leather	QY	70 ± 0.8	−4 ± 0.9	34 ± 1	—	66 ± 0.7	−1 ± 0.9	48 ± 0.2	—
	QY-Si–OH	68 ± 0.4	−4 ± 0.1	51 ± 0.1	17.1 ± 0.2	69 ± 0.1	−3 ± 0.1	53 ± 0.1	4.5 ± 2
	QY-Si–acrylate	72 ± 0.6	−5 ± 0.2	50 ± 0.3	16.1 ± 0.4	74 ± 0.3	−7 ± 0.5	61 ± 0.4	9 ± 1
Vegetable tanned leather	QY	74 ± 0.9	−6 ± 0.2	45 ± 0.2	—	69 ± 0.9	−4 ± 0.1	42 ± 0.5	—
	QY-Si–OH	76 ± 0.1	−6 ± 0.9	41 ± 0.2	6.2 ± 0.6	77 ± 0.2	−8 ± 0.4	39 ± 0.3	9.4 ± 1
	QY-Si–acrylate	68 ± 0.1	−3 ± 0.2	51 ± 0.3	16.4 ± 0.2	72 ± 0.2	−4 ± 0.1	54 ± 0.1	12.4 ± 1

[a] L – lightness, $+a^*$ (positive) – redness, $-a^*$ (negative) – green, $+b^*$ (positive) – yellow, $-b^*$ (negative) - blue.

the same structure was not found in the case of silica nanoparticles with a hydroxyl terminal.[36] The quinoline yellow formed a hollow structure with a mesoporous silica shell, containing a hollow interior (Fig. 1b and c). The shell had a thickness of 18 nm, and the core had different sizes depending on the size of the micelles formed at the initial stage. From the study in the literature on making mesoporous silica using pluronic surfactants, it was reported that the silicate species tend to polymerise in the methyl region of the pluronic surfactants. Hence, in the case of acrylate-based silica precursors, it suggests that silica deposits on the micelles in a similar fashion, leading to the formation of hollow spheres (Scheme 1). Hollow particles were made of individual micellar particles, with ultrafine, primary silica particles deposited outside the core region of the micelles.

It divulges from Fig. 1(a) and (b) that the morphologies of silica nanoparticles with different terminals were different.[37] The particle size obtained from photon correlation spectra in the case of silica spheres indicates the uniform size distribution and monodispersity of the spherical-shaped particles, as shown in Table 1. Additionally, the negative surfaces of the silica nanoparticles had a zeta potential ranging from −48 to −49 mV for Si–OH and from −26 to −15 mV for Si–acrylate. The polydispersity index of the modified dyes reveals monodispersity after surface characterisation using silica with a narrow size distribution. Similarly, the dye modified with silica containing the acrylate bridge showed a uniform size distribution. The variation in dye type has no statistically significant effect on the average diameter of dye-modified silica nanoparticles ($H_0 = 0$, $P > 0.05$). However, the free and dye modified with silica nanoparticles showed a considerable difference ($H_1 = 1$, $P < 0.001$).

UV absorbance spectra of the dye and the dye modified with silica nanoparticles were acquired, as shown in Fig. 1d. In the case of quinoline yellow, the maximum absorbance of 414 nm corresponds to the mono, di and tri sulfonates of 2-(2-quinolyl)-indan-1,3-dione. Charges exchanged between the silica shell and dye molecules induced changes in the chromophore's dielectric constant. Fig. 1(d) clearly demonstrates that the maximum absorbance did not undergo any shift after being modified into the silica matrix but showed slight changes in the scattering intensity owing to the colloidal behaviour of the silica nanoparticles.

The FTIR technique was performed to explore the changes in the surface functional groups of dye molecules before and after silica modification and also to monitor the complete hydrolysis of the silica precursor. The FT-IR spectra of bare dye were compared with dye-modified silica nanoparticles anchored with OH and acrylate groups (as shown in Fig. 1(e)). The spectra of all dyes modified with silica revealed Si–O–Si stretching bands at 1090 cm^{-1} and 830 cm^{-1}. Similarly, the complete hydrolysis of silica precursors was confirmed by the disappearance of a peak ($Si–O–CH_3$) at 2100–2380 cm^{-1}.[38] According to the literature,[39,40] the transverse and longitudinal optical modes of the Si–O–Si asymmetric stretching vibrations were responsible for the intense and wide band at 1104 cm^{-1} and the shoulder around 1198 cm^{-1}. Furthermore, the silica anchored with acrylate

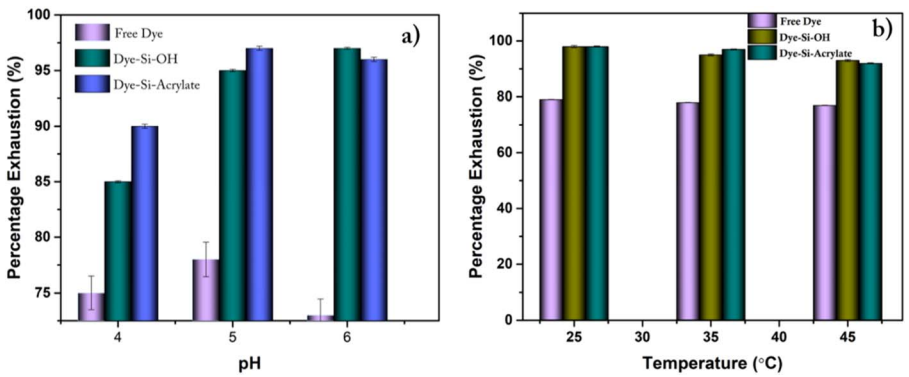

Fig. 4 Effect of temperature and pH on percentage dye exhaustion.

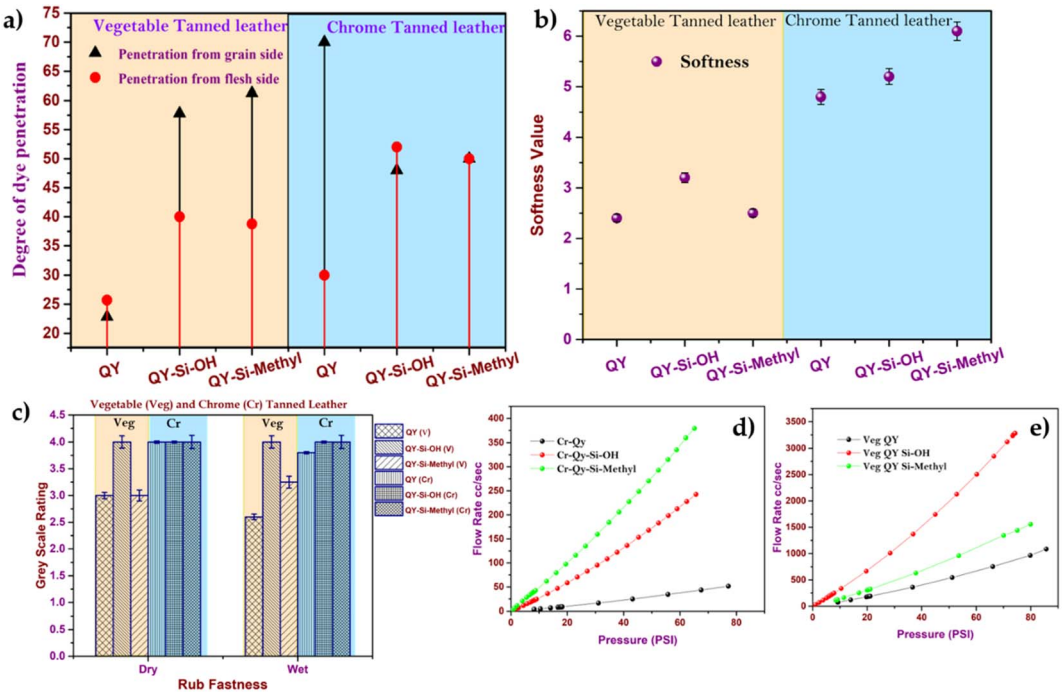

Fig. 5 (a) Degree of dye penetration, (b) softness, (c) rub fastness and (d) and (e) air permeability of the chrome and vegetable-tanned leather.

showed a slight difference with the lack of a C=C peak at 1650 cm^{-1}, which signifies the complete polymerisation of the acrylate group.

Considering the IR pattern of quinoline yellow dye (Fig. 1(e)), the major characteristics of the bands at 660 cm^{-1}, 836 cm^{-1}, 1035 cm^{-1},1199 cm^{-1}, 1351 cm^{-1}, 1421 cm^{-1}, 1538 cm^{-1}, 1644 cm^{-1}, and 3457 cm^{-1} represent the $-NH_2$ wagging, C–H out of plane bending, CCC trigonal bending, C–H inplane bending, C–C stretching, C=N stretching, C=C stretching and N–H asymmetric stretching, respectively. The major structural differences among the free QY dye and QY-supported silica nanoparticles remain at 1035 cm^{-1} and 1199 cm^{-1}, corresponding to the Si–OH interaction towards the dye molecule. It can be clearly observed that after modification with silica (Fig. 1e), the area under the bands at the range of 1215–1230 cm^{-1} is broader owing to the Si–O–Si presence peak

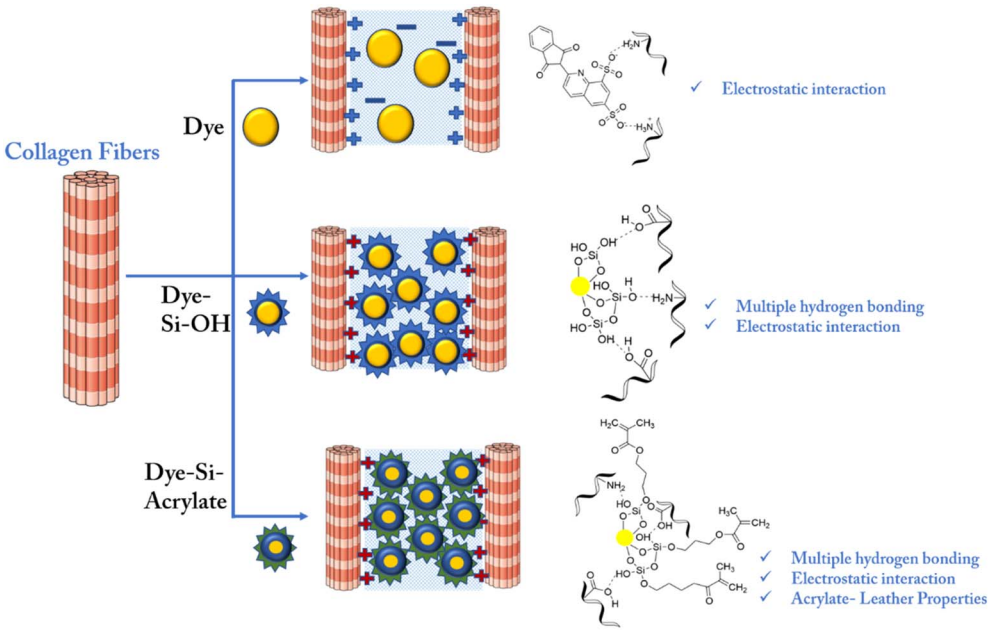

Scheme 2 Interactions between dye and collagen, dye-Si–OH and collagen, dye-Si–acrylate and collagen.

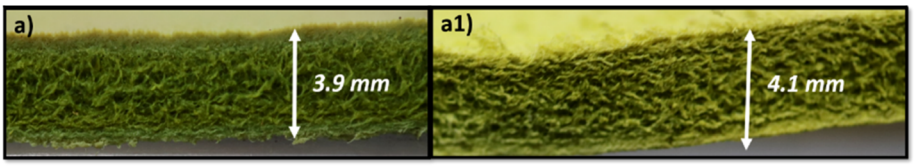

Fig. 6 The cross-sectional view of (a) chrome-tanned leather and (a1) vegetable-tanned leather dyed with dye-modified silica nanoparticles.

merged with the C–H bending of the dye molecules. The characteristic bands at 2927 cm^{-1} and 2834 cm^{-1} are related to the stretching vibrations of the CH_2-groups. The slight deformation of Si–O–Si bands at ranges of 1000–1200 cm^{-1} and 3000–3750 cm^{-1} was identified in the acrylate-attached silica, which can be indicative of a bonding interaction between the dye and SiO_2.

By comparing the IR spectra of dye and dye-modified silica nanoparticles, it was found that the IR spectrum absorption frequencies of the silica functionalization showed slight differences owing to the physical interaction of individual dye molecules. Furthermore, FTIR confirmed that the presence of hydroxyl groups in silica nanoparticles resulted in greater interaction with skin protein, indicating that the modification with silica nanoparticles might be responsible for the good colouring of leather.

The influence of pH and temperature on dye stability and colour (absorbance) was explored, as shown in Fig. 2(a)–(f). After being linked to silica nanoparticles, the dye stability was considerably increased. As inferred from Fig. 2(a)–(c), the particle diameter of the dye-modified silica nanoparticles showed variation in increasing or decreasing trends from their initial diameter with respect to temperature. In the case of dye modified with silica containing hydroxyl terminal (Fig. 2(b)), minimal variation in the *Z*-average was observed with respect to temperature. However, the case of dye modified with silica containing methylacrylate groups (Fig. 2(c)) showed a continuous increase in the *Z*-average with respect to temperature. This may be attributed to the increase in temperature, which causes the methacrylate group to grow in size by the accretion of surface methacrylate molecules with hydroxyl groups available on the other sides of silica. The *Z*-average of the free dyes (Fig. 2(a)) showed a higher rate of aggregation compared with the dye stabilised with silica. Such aggregation leads to poor diffusion of the molecules from the solution to the leather matrix. The DLS measurements demonstrated that dyes modified with silica shells were more stable than free dyes at different temperatures.[41] This can be understood that the dye molecules possessing the conjugated functional groups could quickly form aggregates and even assemblies, leading to dye decomposition. However, in dye-modified systems, the silica on the surface prevents heat from directly reaching the dye and assists in heat dissipation.

In the second step of the stability analysis, the changes in the average diameter of the particles upon the addition of formic acid/sodium bicarbonate were analysed. The dye-modified silica nanoparticle system showed a well-dispersed state, as silica attachment protects the dye from external environmental factors.[42] Quinoline yellow, without an encapsulation system, displayed noticeable size variations (Fig. 2d and e) owing to the direct exposure of the dye molecules. At a pH above 7, the free OH^- ions present in the solution compete with the dye molecule, changing the size of the dye molecules.

The thermal stability of a solution of free dyes and dye-modified silica nanoparticles was investigated by heating each component to temperatures ranging from 20 to 90 °C in a Peltier system chamber (while keeping all other parameters constant) and recording the resulting absorption spectra (as shown in Fig. 2(f)). The results show that the dye-modified silica nanoparticles did not show any change in maximum absorbance, indicating that the dye was stabilised by polymeric silica even at higher temperatures. Owing to direct contact with the

Table 3 Greenness of the developed fatliquoring agent

Parameters	Control process	Experimental process
Environmental	High coloured discharge and poor compatibility between post tanning chemicals Toxic dyes in the effluent	Environmentally friendly chemicals were selected for product preparation Dye exhaustion rate of more than 98% Reduction in pollution load
Social	Leaching of unreacted azo dyes into the wastewater causes an anthropogenic effect	As per FDA (Food and Drug Administration), silica is considered to be safe. Because of modification with silica, there is no leaching of the dye into wastewater
Economical	Using auxiliaries increases the dyeing cost	Reduction in cost and energy owing to the avoidance of dyeing auxiliaries
E factor	0.7	0.35
PMI	5.8	3.96
Dye percentage in wastewater	35–40%	5–12%

Table 4 Economic benefit analysis for producing one ton of dyed leather

Name of the chemicals	Traditional leather dyeing (cost in USD)	Leather dyeing using dye modified with silica (cost in USD)
Sodium bicarbonate	3.06	—
Sodium formate	6.12	—
Dye	458.87	474.16
Dye levelling agent	30.59	—
Fixing agent	36.71	—
Total cost	535.35	474.16

outside environment, a steady decline in their absorbance maxima was observed in the free dye system. As depicted in Fig. 2(f), silica with an acrylate terminal showed higher stability than the hydroxyl terminal owing to the long alkyl chain in the methacrylate group. Hence, leather dyed with dye-modified silica showed higher colour stability under thermal conditions during the product manufacturing process. The more intact the dye molecules survive, the more the original colour is preserved. However, dye-modified silica nanoparticles showed the least changes in the degradation profile, and more than 90% of the dye molecules survived. The presence of silica showed better resistance to fading than free dye because silica can absorb UV energy and dissipate it into heat energy.

Similarly, the stability of the dye-modified silica nanoparticles against various pH values was analysed, as shown in Fig. 3a and b. For all cases, the particle size measurement remained constant, indicating no loss of dye molecules after encapsulation. Adding acid to modified dyes resulted in minimal coalescence, whereas alkali treatment resulted in high stability, which agrees with the reported hydrodynamic size.

Consequently, it can be concluded that functionalizing dye with silica significantly increases dye stability against the outer physiological environment. Additional benefits of the silica matrix include relative inertness or minimal chemical interaction, transparency, heat protection of the dye core, oxidation resistance, and strong mechanical resistance. The dye functionalized with silica is non-toxic and biocompatible, making it appropriate for leather dyeing applications.

To understand dyeability, the vegetable-tanned and chrome-tanned leathers were dyed with silica-based dyes. Fig. S3† shows the vegetable-tanned leather dyed with both free and the dye modified with silica nanoparticles. Fig. S3† illustrates that the leather dyed with free quinoline yellow (anionic dye) shows non-uniform penetration of dye on the entire cross sections. Non-uniform penetration occurs due to the variation in charge of the leather. In addition, the presence of high molecular weight polyphenols (vegetable tannins) inhibits dye penetration. The dye-modified silica nanoparticle system showed excellent penetration of anionic dyes on the inner surface at a faster rate. According to the literature,[43] when dye-modified silica nanoparticles dispersed in the polyphenol solution, –OH groups on them interacted with polyphenols (vegetable tannins) through hydrogen bonding. Hence, it is evident that the dyeing characteristics of anionic dyes towards vegetable-tanned leather improved significantly because of the presence of silica with a hydroxyl functional group. In contrast, silica with an acrylate functional group showed better dyeing characteristics for chrome-tanned leather than for vegetable-tanned leather.

Fig. S2† shows chrome-tanned crust leathers dyed using the anionic dye quinoline yellow, and Fig. S3† shows the vegetable-tanned crust leathers dyed using quinolone yellow dye. Chrome-tanned leather showed through and through dye penetration as well as uniform surface colour. It was observed from Fig. S2† that the modified dyes showed excellent surface color characteristics compared with the free dye system. Additionally, the grain and flesh surface of the crust leathers showed uniform surface colour and even penetration of dyes. Using a modified system, the variation in colour difference is minimised. It is also evident from the colour coordinate measurement of dyed leather (Table 2) that there was a slight variation in L values between free and dye-modified silica-treated leather. The percentage of dye exhaustion was in the range of 95–98% for leather dyed with dye modified with silica compared to leathers treated with free dye (79%). The effects of dyebath pH and temperature on percentage dye exhaustion were monitored, as presented in Fig. 4a and b. The percentage of dye exhaustion increased with the increase in dye bath pH. Silica with acrylate showed a high exhaustion rate at high temperatures compared to silica with hydroxyl group and free dyes. The optimum temperature was found to be in the range of 25–30 in the case of silica with hydroxyl and methacrylate terminal. Similarly, high exhaustion was obtained at the pH range of 5–6 in both hydroxyl and methacrylate terminals. To avoid leaching of other post tanning chemicals, the dyeing bath pH was varied only from 4 to 6.

The variations in dye penetration to vegetable and chrome-tanned leather were studied, as shown in Fig. 5a. Silica with acrylate terminal showed lower penetration through the flesh side of vegetable-tanned leather (Fig. 5a) than the grain side. This lower penetration through the flesh side was due to the weaker interaction of acrylate with vegetable tannins. However, the smaller particle size of dye-modified silica was adsorbed rapidly through the grain side. Hence, the narrow size distribution of dye-modified silica nanoparticles (~50–80 nm) easily penetrates inside the highly filled vegetable-tanned leather and has proper dye distribution, leading to uniform colour on the grain side. However, silica with a hydroxyl group showed uniform penetration on both the flesh and grain sides of the chrome-tanned leather. The presence of silica may influence the softness property of the tanned, so the softness of vegetable-

tanned leather and chrome-tanned leather dyed with silica dyes were compared, as shown in Fig. 5b. From Fig. 5b, it was confirmed that the dye modified with silica-treated chrome-tanned leather was softer than vegetable-tanned leather. The obtained high softness value (Fig. 5b) was mainly due to the porous structure of silica responsible for the increase in softness and smoothness of the grain with a less uneven coating over the surface. Hence, this proves that the dye-modified silica nanoparticles improve the uniform distribution of oil inside the leather matrix and that the presence of silica enriches the leather softness property.

In most of the experiments, leathers coloured with surface-modified dye had a wet rub fastness range of 4–5, demonstrating that the developed dye had a stronger binding to the leather. Water is used to test the resistivity of coloured leather, such as colour transfer against water (Table S3†). Because the framed silica structure easily absorbs the unfixed dye released, the greyscale assessment revealed that all surrounding fabrics experienced less colour transfer.[44] Resistance against colour transfer is also attributed to the presence of many hydroxyl groups on the nanoparticle surface, which minimizes silica-leather dissociation and provides a superior fastness property.[45]

The air permeability of the leather after being treated with dye-modified silica nanoparticles was measured to estimate the filling properties offered by silica nanoparticles. The curve of flow rates as a function of the applied pressure is shown in Fig. 5(d) and (e). Higher permeation resistance was observed in the case of dye-modified silica nanoparticles (dye-silica–acrylate) treated leather than in the free dye system. Pan *et al.*[25] reported that applying nano-SiO_2 as a retanning agent imparts fullness and improves the leather's physical properties. In this study, it is observed that the uniformity of the leather is significantly enhanced by the presence of silica.[46] The dye-modified silica nanoparticles were evenly dispersed in the leather matrix owing to the small particle size, thereby improving the overall leather texture and cutting value. The SEM (Scanning Electron Microscope) image of dye-modified silica nanoparticles adhered to leathers, which showed a highly compact fibre direction with a smooth uniform surface, supported uniform dye-modified silica nanoparticle distributions (Fig. S4†). The dual advantage of obtaining excellent dyeing characteristics and the improved physical properties impulse the new dyeing-modified silica nanoparticle system to be superior to the conventional dyeing system.

Leathers were placed on hot metallic surfaces for 5 seconds to investigate the durability of coloured leather against heat. The temperature of hot metallic surfaces is maintained at 50, 100, 150, 200, and 250 °C (Table S4†) to elucidate the rate of colour change. The decrease in the greyscale rating of free conventional dye-treated leathers suggests that the supplied heat breaks the ionic contact between the dye and matrix. However, the temperature did not affect the dye modified with silica because of the enormous energy required to break the high silica network structure.[47–49] As shown in Table S4,† the functionalization of the dye surface significantly improves heat resistance, suggesting that the dye-modified silica system is a novel material for dyeing fibrous matrices with good resistance to heat during application.

This improvement in heat resistance may be due to the multiple bonding between the silica terminal and leather matrix. Considering the interaction mechanism between collagen and dye, dye alone forms only an electrostatic interaction with leather based on the charge availability. However, dye-modified silica with hydroxyl terminals forms multiple hydrogen bonds, van der Waals forces, and other non-covalent forces with the amino, hydroxyl, carboxyl, and amide groups present on the side chains of leather collagen, as shown in Scheme 2. However, silica with both hydroxyl and acrylate terminals enhances leather properties through preferential filling, followed by multiple hydrogen bonding.

To understand whether the uniform colour adsorption was due to decreased particle size or accessible functional groups, dye adsorption over a 4 mm leather thickness was performed (Fig. 6). Uniform dye penetration demonstrated that both particle size and the structure of silica containing functional groups affected adsorption capabilities, as evidenced by decreased variation in dye dispersion across the full matrix thickness (3.8–4 mm).

The elemental analysis for both free and dye-modified silica nanoparticle-treated leathers was attempted to visualise the dye transportation through silica attachment towards leather. From Fig. S5–S7,† silica is present at the inner cross-section of the experimental leather, as the dye-modified silica penetrates more evenly compared to traditional free dyes. Hence, it is concluded that the dye modified on silica improves the dyeing based on the size as well as charge irrespective of substrate characteristics.

Sustainable impact assessment

The objective of this study is to replace conventional anionic dyes with nanoparticle-assisted dying agents to improve leather performance in terms of leather quality and the high uptake of dyes with less dye leaching into wastewater. The greenness of using dye modified with silica as a dyeing agent in the leather dyeing process is summarized, as depicted in Table 3.

The equation for finding E factor[50] (Environmental factor) and PMI[51] (Process Mass Intensity) is listed in Fig. ESI eqn. (1) and (2),† respectively. Compared to the control process, the E factor of the experimental process was estimated to be lower (at a value of 0.35), indicating the minimum organic load discharged from the experimental process. The microemulsion technique was used to prepare dye modified with silica nanoparticles. Water is used as the solvent. The mass intensity was estimated to be 3.96 in the case of dye modified with a silica system compared to conventional dyeing (5.8). Further reduction in the mass intensity of the experimental process can be achieved by replacing the silica source (obtained from waste) and avoiding the excessive use of the stabilising agent. Similarly, the amount of dye discharged from conventional and experimental dyeing was analysed, and the values are shown in Table 3. The conventional dyeing system was generally discharging more coloured discharge (containing azo dyes), which

leads to serious health problems. In the case of a new dyeing system, the elimination of auxiliaries and less dye input makes this new silica-based dyeing process environmentally beneficial compared to a conventional system.

Analysis of economic benefits

The cost analysis for dyeing 1 ton of shaved wet blue using traditional dyes modified with silica nanoparticles is presented in Table 4. Owing to the avoidance of auxiliaries, dyeing with dye-modified silica nanoparticles was comparatively cheaper than the traditional dyeing system. In addition, the percentage offer of dyes was also halved compared to the traditional dyeing system. The synergetic benefit of the avoidance of auxiliaries and less percentage offer makes this new dyeing system more economically viable than traditional system in a cost-effective manner. Therefore, the development of environmentally benign and cost-effective dyes modified with silica nanoparticles is very favourable in leather dyeing with less environmental pollution in an economical way.

Relating to sustainability development goals (SDGs)

According to the United National Development Goals (SDGs) for the leather sector, goal 6 clean water and sanitation states that "by reducing the pollution load and minimizing the release of hazardous chemicals and materials, 50% of the untreated wastewater reduces". This leads to a substantial increase in recycling and safe reuse globally. Moreover, a reduction in wastewater discharge improves water quality by supplying fresh water to address water scarcity. This study uses silica-modified dyes as dyeing agents. There is a 50% reduction in the water input and a 35–40% reduction in the coloured discharge of wastewater. Therefore, this new dyeing system is more environmentally friendly than the conventional system owing to its reduced dye discharge into wastewater. Based on sustainable development goals, the new dyeing system generates clean water (can be recycled) compared to conventional dyeing.

Conclusions

In this study, novel dye-modified hollow silica nanoparticles were prepared using modified microemulsion techniques. Two types of dye-modified silica nanoparticles were prepared: one with a hydroxyl functional group and the other with a methacrylate functional group. TEM results confirmed uniform spherical-shaped particle formation with a low polydispersity index in both cases. Under a wide pH range, the dye modified with silica functional groups showed high negative surface charges and narrow hydrodynamic sizes. In leather dyeing, this dye immobilised on a hollow structure was preferred for better binding towards collagen protein. The optimum condition for maximum dye uptake was obtained for both vegetable and chrome-tanned leather at a pH range of 5.5–6, 90 min of drumming and 25–30 °C. Both hydroxyl- and methacrylate-based dye-modified silica were used for dyeing chrome and vegetable-tanned leathers. Silica with a hydroxyl group showed good dyeing properties, such as dye penetration, fastness and exhaustion, with vegetable-tanned leather. Similarly, silica with methacrylate showed good dyeing characteristics with chrome-tanned leather. Using these silica-modified dyes, the E factor (environmental factor) of the new way of dyeing by hollow nanoparticles was found to be lower, indicating minimum emissions and less pollution load. Additionally, silica-modified dyes reduce the amounts of dyes released into wastewater compared to the conventional dyeing process. Hence, it was easy to treat the wastewater at a lower capital. In the conventional dyeing process, more dyes and auxiliaries were used to produce good quality leather. However, in the newer process, a lower percentage of dyes and the avoidance of auxiliaries were obtained with dye modified with silica nanoparticles. Reduction in the mass intensity compared with the control process contributes to the generation of a sustainable dyeing process.

Author contributions

S. R. performed the experiments. K. J. S. and J. R. R. designed the experiments and corrected the manuscript.

Conflicts of interest

All authors declare that there is no conflicts of interest.

Acknowledgements

One of the authors S. R. wishes to thank the DST-INSPIRE, New Delhi, for providing a Senior Research Fellowship GAP 1403. The authors would like to thank Centre for Analysis, Testing, Evaluation& Reporting Services (CATERS), CLRI for the testing facility. CSIR-CLRI communication no. 1660.

References

1 A. Aslan, *Ekoloji*, 2013, **22**, 26–35.
2 Y. Chu, N. Corrigan, C. Wu, C. Boyer and J. Xu, *ACS Sustainable Chem. Eng.*, 2018, **6**, 15245–15253.
3 S. Te Lin, T. H. You and C. Cheng, Method for reactive dyeing of leather, *US Pat.*, US20070033746A1, 2012.
4 H. Zeng and R.-C. Tang, *RSC Adv.*, 2014, **4**, 38064–38072.
5 J. z. Ma, Q. Liu, M. Wu and Z. Tian, Preparation and assistant-dyeing of formaldehyde-free amphoteric acrylic retanning agent, *J. Leather Sci. Eng.*, 2021, **3**(1), 26.
6 B. Lellis, C. Z. Fávaro-Polonio, J. A. Pamphile and J. C. Polonio, *Biotechnol. Res. Innov.*, 2019, **3**, 275–290.
7 H. Andrew, Leather Dyeing, WO2000077292A1, 2000.
8 F. E. Atteaux, *J. Ind. Eng. Chem.*, 1910, **2**, 218–219.
9 G. Hussain, M. Ather, M. U. A. Khan, A. Saeed, R. Saleem, G. Shabir and P. A. Channar, *Dyes Pigm.*, 2016, **130**, 90–98.
10 F. L. Labarthet, J. L. Bruneel, T. Buffeteau and C. Sourisseau, *J. Phys. Chem. B*, 2004, **108**, 6949–6960.
11 A. D. Covington, *Tanning Chemistry the Science of Leather*, 2009.
12 R. S. Dietrich Lach and F. Feichtmayr, Dyeing of grain leather, *US Pat.*, US4272243A, 1978.
13 A. A. Haroun and H. F. Mansour, *Dyes Pigm.*, 2007, **72**, 80–87.

14 G. Krishnamoorthy, S. Sadulla, P. K. Sehgal and A. B. Mandal, *J. Cleaner Prod.*, 2013, **42**, 277–286.
15 V. Sivakumar, G. Swaminathan, P. G. Rao, C. Muralidharan, A. B. Mandal and T. Ramasami, *Ultrason. Sonochem.*, 2010, **17**, 1054–1059.
16 S.-S. Sun, T. Xing and R.-C. Tang, *Ind. Eng. Chem. Res.*, 2013, **52**, 8953–8961.
17 R. K. Sharma, S. Sharma, S. Dutta, R. Zboril and M. B. Gawande, *Green Chem.*, 2015, **17**, 3207–3230.
18 T. Uemura, Y. Kadowaki, C. R. Kim, T. Fukushima, D. Hiramatsu and S. Kitagawa, *Chem. Mater.*, 2011, **23**, 1736–1741.
19 L. Pena, K. Hohn, J. Li, X. Sun and D. Wang, *J. Biomater. Nanobiotechnol.*, 2014, **05**, 241–253.
20 M. Montalti, L. Prodi, E. Rampazzo and N. Zaccheroni, *Chem. Soc. Rev.*, 2014, **43**, 4243–4268.
21 H. Ow, D. R. Larson, M. Srivastava, B. A. Baird, W. W. Webb and U. Wiesner, *Nano Lett.*, 2005, **5**, 113–117.
22 T. Okada and T. Koide, *Langmuir*, 2018, **34**, 9500–9506.
23 L. S. Ribeiro, T. Pinto, A. Monteiro, O. S. G. P. Soares, C. Pereira, C. Freire and M. F. R. Pereira, *J. Mater. Sci.*, 2013, **48**, 5085–5092.
24 T. Ribeiro, C. Baleizão and J. P. S. Farinha, *J. Phys. Chem. C*, 2009, **113**, 18082–18090.
25 H. Pan, G.-L. Li, R.-Q. Liu, S.-X. Wang and X.-D. Wang, *Appl. Surf. Sci.*, 2017, **426**, 376–385.
26 E. Claesson and A. Philipse, *Colloids Surf., A*, 2007, **297**, 46–54.
27 Y. Liang and R. Pearson, *Polymer*, 2009, **50**, 4895–4905.
28 H. Pu, X. Zhang, J. Yuan and Z. Yang, *J. Colloid Interface Sci.*, 2008, **331**, 389–393.
29 R. P. Bagwe, L. R. Hilliard and W. Tan, *Langmuir*, 2006, **22**, 4357–4362.
30 H. Wang, J. Fang, T. Cheng, J. Ding, L. Qu, L. Dai, X. Wang and T. Lin, *Chem. Commun.*, 2008, **7**, 877–879.
31 C. Malba, U. Sudhakaran, S. Borsacchi, M. Geppi, F. Enrichi, M. Natile, L. Armelao, T. Finotto, R. Marin, P. Riello and A. Benedetti, *Dalton Trans.*, 2014, (43), 16183–16196.
32 H. Liang, C. Jin, Y. Tang, F. Wang, C. Ma and Y. Yang, *J. Appl. Toxicol.*, 2014, **34**, 367–372.
33 S. Bhattacharjee, *J. Controlled Release*, 2016, **235**, 337–351.
34 IUP 2, Sampling, *J. Soc. Leather Technol. Chem.*, 2000, **84**(2), 303–308.
35 R. Naffa, C. Maidment, M. Ahn, B. Ingham, S. Hinkley and G. Norris, *Int. J. Biol. Macromol.*, 2019, **128**, 509–520.
36 E. Yamamoto and K. Kuroda, *Enzymes*, 2018, **44**, 1–10.
37 M. A. Khan, W. T. Wallace, S. Z. Islam, S. Nagpure, J. Strzalka, J. M. Littleton, S. E. Rankin and B. L. Knutson, *ACS Appl. Mater. Interfaces*, 2017, **9**, 32114–32125.
38 S. Islam, H. Bakhtiar, W. N. W. Shukri, M. S. a. Aziz, S. Riaz and S. Naseem, *Microporous Mesoporous Mater.*, 2019, **274**, 183–189.
39 H. Omranpour and S. Motahari, *J. Non-Cryst. Solids*, 2013, **379**, 7–11.
40 S. A. Mahadik, F. Pedraza, V. G. Parale and H.-H. Park, *J. Non-Cryst. Solids*, 2016, **453**, 164–171.
41 X. Zhou and J. Zhou, *Anal. Chem.*, 2004, **76**, 5302–5312.
42 A. Ahmad, N. D. Zakaria, Z. Lockman and K. A. Razak, *AIP Conf. Proc.*, 2018, **1958**, 020010.
43 Y. Bao, J. Z. Ma, J. L. Liu and J. Lu, *J. Soc. Leather Technol. Chem.*, 2013, **97**, 238–243.
44 Z. S. a. A. Shahbazi, *Eur. J. Environ. Saf. Sci.*, 2014, **4**, 116–130.
45 A. Hudson, *J. Soc. Dyers Colour.*, 2000, **116**, 310–315.
46 L. L. Haojun Fan, Bi Shi, H. E. Qiang and B. Y. Peng, *J. Am. Leather Chem. Assoc.*, 2005, **100**, 22–30.
47 S. H. Joo, J. Y. Park, C.-K. Tsung, Y. Yamada, P. Yang and G. A. Somorjai, *Nat. Mater.*, 2009, **8**, 126–131.
48 G. M. Veith, A. R. Lupini, S. Rashkeev, S. J. Pennycook, D. R. Mullins, V. Schwartz, C. A. Bridges and N. J. Dudney, *J. Catal.*, 2009, **262**, 92–101.
49 V. Arabli and A. Aghili, *Adv. Compos. Mater.*, 2014, 1–17, DOI: **10.1080/09243046.2014.944254**.
50 R. A. Sheldon, *Green Chem.*, 2017, **19**, 18–43.
51 A. P. C. Ribeiro, L. M. D. R. S. Martins, D. E. N. Bastos, A. F. Cristino and R. Galhano dos Santos, *Handbook of Greener Synthesis of Nanomaterials and Compounds*, ed. B. Kharisov and O. Kharissova, Elsevier, 2021, pp. 37–62, DOI: **10.1016/B978-0-12-821938-6.00002-5**.